

Solvent-Free Approach for Interweaving Freestanding and Ultrathin Inorganic Solid Electrolyte Membranes

Changhong Wang,^{II} Ruizhi Yu,^{II} Hui Duan,^{II} Qingwen Lu, Qizheng Li, Keegan R. Adair, Danni Bao, Yang Liu, Rong Yang, Jiantao Wang*, Shangqian Zhao*, Huan Huang*, and Xueliang Sun*



Cite This: *ACS Energy Lett.* 2022, 7, 410–416



Read Online

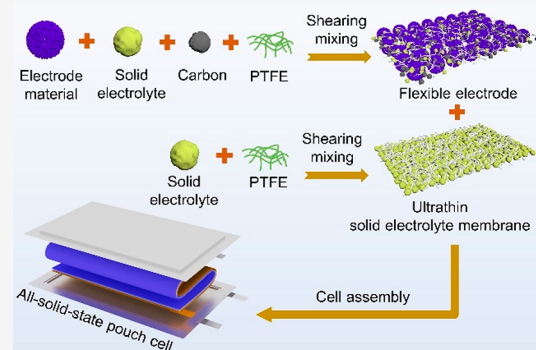
ACCESS |

Metrics & More

Article Recommendations

Supporting Information

ABSTRACT: All-solid-state batteries (ASSBs) have gained considerable attention due to their inherent safety and high energy density. However, fabricating ultrathin and freestanding solid electrolyte membranes for practical all-solid-state pouch cells remains challenging. In this work, polytetrafluoroethylene (PTFE) fibrilization was utilized to interweave inorganic solid electrolytes (SEs) into freestanding membranes. Representative SE membranes, including $\text{Li}_6\text{PS}_5\text{Cl}$, Li_3InCl_6 , and $\text{Li}_{6.5}\text{La}_3\text{Zr}_{1.5}\text{Ta}_{0.5}\text{O}_{12}$, demonstrate not only a thickness of 15–20 μm but also high room-temperature ionic conductivity ($>1 \text{ mS cm}^{-1}$). All-solid-state pouch cells with bilayer $\text{Li}_6\text{PS}_5\text{Cl}$ and Li_3InCl_6 membranes deliver a high capacity of 124.3 mAh g^{-1} at 0.1 C and an initial Coulombic efficiency of 89.4%. Furthermore, using a 20 μm LLZTO membrane as a ceramic separator, a solid-state pouch cell with a high-capacity $\text{LiNi}_{0.8}\text{Mn}_{0.1}\text{Co}_{0.1}\text{O}_2$ electrode ($>3 \text{ mAh cm}^{-2}$) displays both exceptional cycling stability and unprecedented safety. We believe that this solvent-free technology would be a feasible and cost-effective means of transferring ASSB technology from the laboratory to the factory.



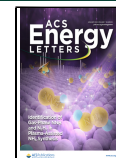
Lithium-ion batteries (LIBs) have dominated the consumable electronic market for 30 years and have become a vital source of power for electric vehicles (EVs) and grid-scale energy storage.¹ However, conventional LIBs use flammable liquid electrolytes and combustible organic polymer separators, which pose a safety risk in use. In addition, their energy density is gradually approaching their theoretical limits. Under this circumstance, developing all-solid-state batteries (ASSBs) by replacing the flammable liquid electrolyte and organic separator with inorganic solid electrolytes has been considered a strategic way to enhance energy density and safety spontaneously.² The past decade has witnessed a rapid development of various solid-state electrolytes (SEs), such as polymer electrolytes,^{3–6} sulfide electrolytes,^{7–9} oxide electrolytes,¹⁰ halide electrolytes,^{11–15} borohydrides,¹⁶ antiperovskites,¹⁷ and their composites.^{18,19} Some ASSBs demonstrated in the laboratory have shown unparalleled electrochemical performance and unprecedented safety.^{7,8,20} Despite these encouraging advances, the commercialization of ASSBs has remained stagnant, which is due to the lack of a feasible technology to fabricate ultrathin inorganic SE membranes without compromising their high ionic conductivity.^{21–23}

To date, two methods have been attempted to fabricate SE membranes: i.e., high-vacuum deposition and tape casting. The former includes pulsed laser deposition (PLD), chemical vapor deposition (CVD), and radio frequency (RF) magnetron sputtering.^{22,24} These high-vacuum deposition techniques, however, are impractical for the mass production of large-capacity all-solid-state pouch cells because of their high cost and low production efficiency. The latter technique has been widely demonstrated to fabricate inorganic ceramic membranes (e.g., 25–41 μm $\text{Li}_{0.34}\text{La}_{0.56}\text{TiO}_3$,²⁵ 75 μm $\text{Li}_{1.4}\text{Al}_{0.4}\text{Ge}_{1.6}(\text{PO}_4)_3$,²⁶ and bilayer and trilayer $\text{Li}_3\text{La}_{2.75}\text{Ca}_{0.25}\text{Zr}_{1.75}\text{Nb}_{0.25}\text{O}_{12}$ ^{27,28}), inorganic/organic hybrid membranes (e.g., SE in a polymer matrix (SEPM)²⁹ and $\text{Li}_{6.5}\text{La}_3\text{Zr}_{1.5}\text{Ta}_{0.5}\text{O}_{12}$ (LLZTO) on PP separators³⁰), and pure polymer electrolytes (e.g., PEO/LiTFSI in PI film³¹). In a typical tape-casting process, solvents,

Received: October 16, 2021

Accepted: December 21, 2021

Published: December 27, 2021



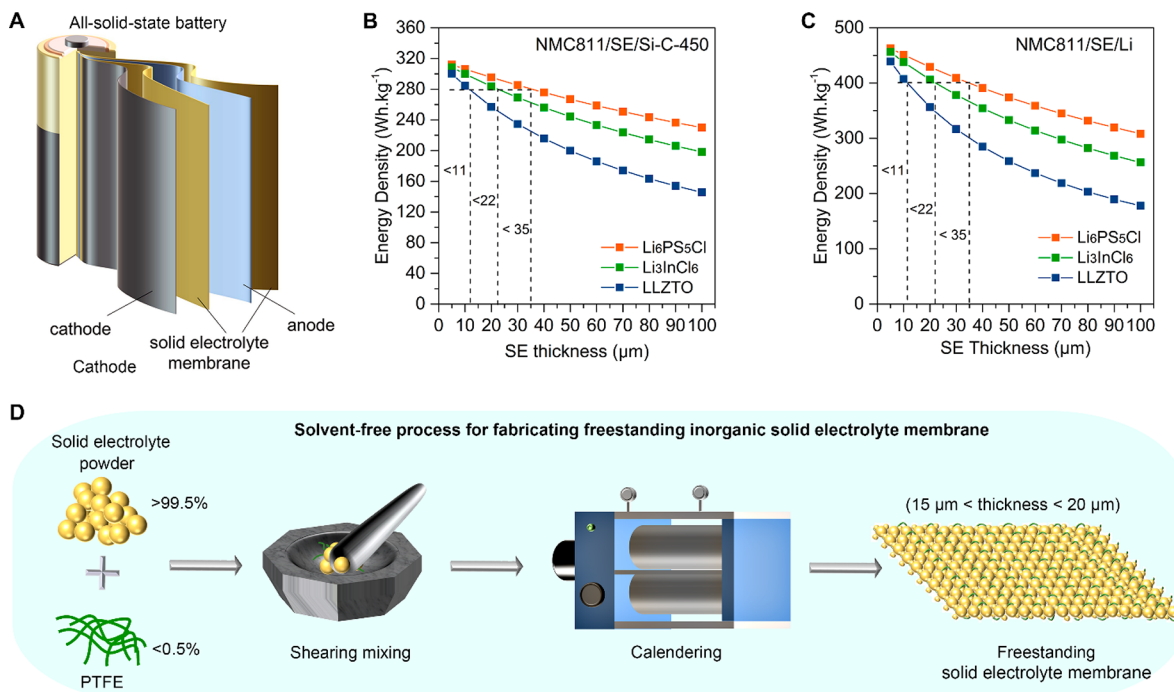


Figure 1. Energy density analysis and illustration of a solvent-free process for fabricating inorganic solid electrolyte membranes. (A) Schematic of a cylindrical solid-state battery. (B) Calculated gravimetric energy density of all-solid-state batteries with a configuration of NMC811|SE|Si-C-450 as a function of SE membrane thickness from 5 to 100 μm . (C) Calculated gravimetric energy density of all-solid-state batteries with a configuration of NMC811|SE|Li as a function of SE membrane thickness from 5 to 100 μm . (D) Schematic of the fabrication process for thin SE membranes.

dispersants, polymeric binders, plasticizers, and inorganic SE particles are mixed to form a slurry and then cast on a substrate.³² However, these polar solvents and binders are detrimental to SEs, particularly chemically vulnerable sulfide and halide electrolytes,^{33–37} thus greatly reducing their ionic conductivity. In addition, a large amount of binder used in the tape-casting process considerably impedes interparticle contacts, thus limiting lithium-ion transport between SE particles. Furthermore, solvent evaporation necessitates an energy-intensive heating process, which is undesirable for zero-emission manufacturing. Given the limitations of the tape-casting and high-vacuum deposition methods, developing a new and viable method to fabricate ultrathin inorganic SE membranes remains crucial and urgent for ASSB commercialization.

In this work, a solvent-free method is reported to fabricate freestanding and ultrathin inorganic SE membranes. Taking advantage of polytetrafluoroethylene (PTFE) fibrilization, the representative sulfide electrolyte Li₆PS₅Cl, halide electrolyte Li₃InCl₆, and oxide electrolyte LLZTO were fabricated into large-sheet membranes ($8 \times 6 \text{ cm}^2$) with a thickness of 15–20 μm . It should be emphasized that this thickness is comparable to that of conventional polymeric separators. Benefiting from the solvent-free process, the high ionic conductivity of inorganic SEs (i.e., Li₆PS₅Cl and Li₃InCl₆) is well kept over 1 mS cm^{-1} . All-solid-state pouch cells based on bilayer ultrathin Li₆PS₅Cl and Li₃InCl₆ membranes were demonstrated and exhibited impressive electrochemical performance. Furthermore, a practical solid-state pouch cell based on a high-loading electrode of LiNi_{0.8}Mn_{0.1}Co_{0.1}O₂ (NMC811; 17.1 mg cm^{-2}) presents a stable cycling performance with an areal capacity of 3 mAh cm^{-2} . We believe the proposed solvent-free method would be a viable and cost-effective way of transitioning ASSB technology from the laboratory to the factory.

Figure 1A illustrates a configuration of a cylindrical ASSB, in which a SE membrane is sandwiched between a cathode and an anode. According to the equation $\tau = l^2/D$, where τ is the Li-ion diffusion time, l is the thickness of the SE layer, and D is the diffusion constant, reducing the thickness of the SE membrane is crucial for high ionic conductance due to shortening the Li⁺ diffusion distance and time. Therefore, reducing the thickness of the SE layer in ASSBs can increase both the energy density and power density spontaneously.^{21,23,38,39} To examine the thickness effect of SEs on the energy density, a numerical analysis was performed with the representative sulfide electrolyte Li₆PS₅Cl, halide electrolyte Li₃InCl₆, and oxide electrolyte LLZTO. The detailed parameters for this numerical calculation are given in Table S1. When typical LiNi_{0.8}Mn_{0.1}Co_{0.1}O₂ (NMC811) is used as the cathode and silicon–carbon (Si–C) composites with a specific capacity of 450 mAh g⁻¹ (Si-C-450) as the anode, an energy density of 280 Wh kg⁻¹ can be realized, providing the thicknesses of Li₆PS₅Cl, Li₃InCl₆, and LLZTO go down to 35, 22, and 11 μm , respectively (Figure 1B). Under the same conditions, the energy density of all-solid-state pouch cells can increase to 305 Wh kg⁻¹ if Si–C composites with a capacity of 600 mAh g⁻¹ are used as the anode (Figure S1), suggesting that increasing the anode capacity is crucial for realizing a high energy density of ASSBs. Furthermore, if Li metal is used as the anode, which has been regarded as the ultimate choice of anodes due to its high theoretical capacity of 3860 mAh g⁻¹ and lowest electrochemical potential (−3.040 V vs the standard hydrogen electrode), the energy density of all-solid-state pouch cells can reach up to 400 Wh kg⁻¹, assuming SE membranes with the same thickness are used (Figure 1C). This numerical analysis leads to two conclusions. First, the thickness of SE membranes should be as thin as possible in order to obtain a high energy density of all-solid-state pouch cells. Second, using high-capacity

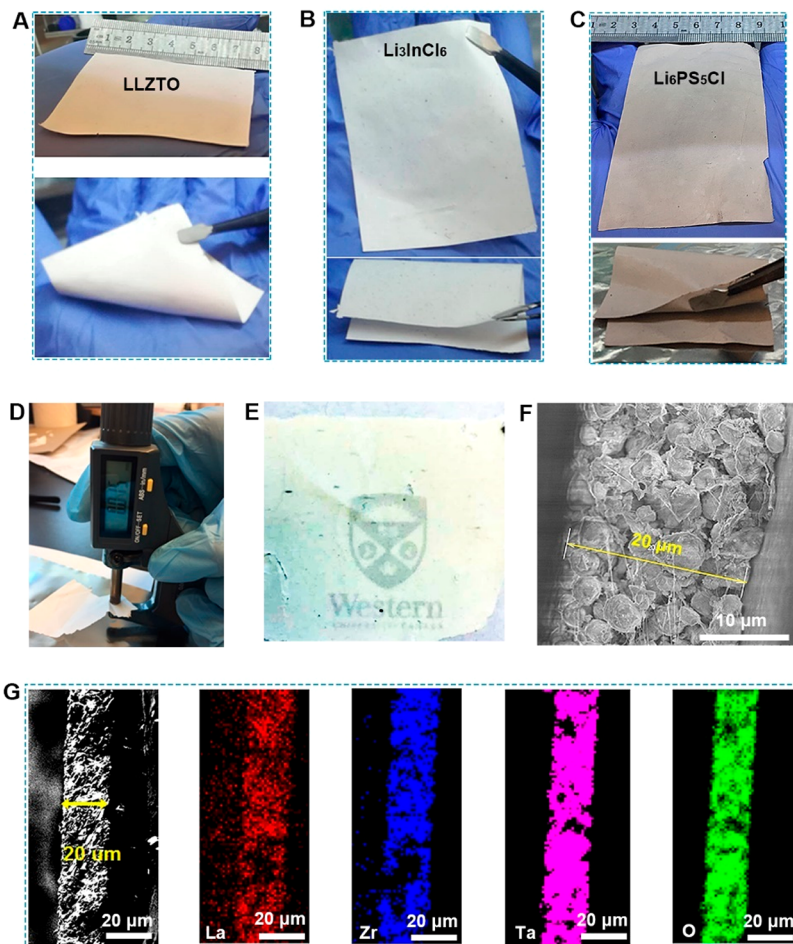


Figure 2. Characterizations of inorganic solid electrolyte membranes. (A) Photo of an LLZTO membrane with a thickness of 20 μm and an area of $8 \times 6 \text{ cm}^2$. (B) Photo of a Li₃InCl₆ membrane with a thickness of 20 μm and an area of $8 \times 6 \text{ cm}^2$. (C) Photo of a Li₆PS₅Cl membrane with a thickness of 20 μm and an area of $8 \times 6 \text{ cm}^2$. (D) Image of a 15 μm LLZTO membrane. (E) Image of a 15 μm LLZTO membrane showing the translucent property. (F) Cross-sectional SEM image of a 20 μm LLZTO membrane. (G) EDS mapping of a 20 μm LLZTO membrane.

anodes such as silicon and Li metal can obtain a higher energy density in comparison to that of traditional liquid-based LIBs. Therefore, fabricating thin SE membranes, while receiving less attention, is of foremost significance for practical ASSBs.

With this understanding, a solvent-free process is proposed herein to fabricate thin and freestanding SE membranes. As shown in Figure 1D, on the basis of the fibrilization of only 0.5 wt % PTFE, 99.5 wt % SE powder can be easily interwoven into a malleable and elastic flake, which can be further pressed into a freestanding membrane with the desired thickness via roll-to-roll pressing. The whole process is solvent-free, scalable, energy-efficient, cost-effective, and compatible with the existing LIB roll-to-roll manufacturing process.⁴⁰ Representative SEs, including the sulfide electrolyte Li₆PS₅Cl, halide electrolyte Li₃InCl₆, and oxide electrolyte LLZTO, were fabricated and are presented in Figure 2.

Figure 2A–D shows the photos of freestanding Li₆PS₅Cl, Li₃InCl₆, and LLZTO membranes with large areas of $8 \times 6 \text{ cm}^2$ and thicknesses of 15–20 μm (Figure S2). Interestingly, the LLZTO membrane becomes translucent when it is pressed to 15 μm (Figure 2E). All of the LLZTO particles are interwoven by PTFE fibers, which is like a “gabion basket”, as illustrated in the cross-sectional scanning electron microscopy (SEM) image of a 20 μm LLZTO membrane (Figure 2F). Its EDS mapping confirms the elemental composition of LLZTO (Figure 2G). To

the best of our knowledge, a 15–20 μm inorganic SE membrane is the thinnest that has been reported so far (Table S2).

Figure 3A–C shows the X-ray diffraction (XRD) patterns of these SE membranes in comparison with their powder form. A well-maintained crystal structure implies that the high ionic conductivity of inorganic SEs is retained. To confirm this, the ionic conductivity of these SE membranes was further measured by electrochemical impedance spectroscopy (EIS) (Figure S3). Although the ionic conductivity of Li₆PS₅Cl powder is as high as 2.4 mS cm^{-1} (Figure 3D), the actual conductance is only 18.9 mS due to its thick thickness. Comparatively, the thin Li₆PS₅Cl membrane has an ultralow resistance of 1.5 Ω , which corresponds to a conductance of up to 666.7 mS . Similarly, the Li₃InCl₆ powder exhibits a high ionic conductivity of 1.5 mS cm^{-1} but a low conductance of 14.2 mS (Figure 3E), while its thin membrane has a high conductance of 394.1 mS . The high conductances of the Li₆PS₅Cl and Li₃InCl₆ membranes are ascribed to two reasons. First, unlike the conventional tape-casting process, this solvent-free process does not involve any polar solvents and binders;^{41,42} thus, the crystal structure and high ionic conductivity of SEs can be well maintained. Second, only a limited amount (0.5%) of nonpolar PTFE is used; thereby the blocking effect of polymeric binders on Li-ion transport between SE particles is considerably minimized.⁴²

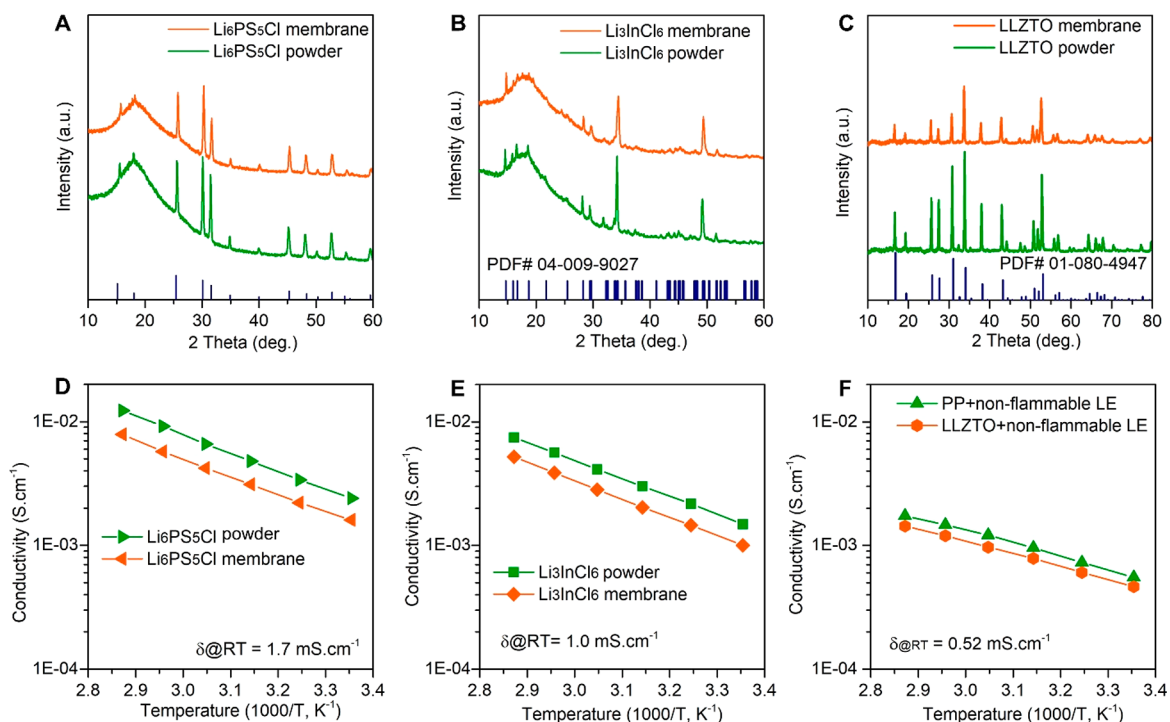


Figure 3. Structural analysis and ionic conductivity of an inorganic solid electrolyte membrane. (A) XRD patterns of $\text{Li}_6\text{PS}_5\text{Cl}$ and its membrane. (B) XRD patterns of Li_3InCl_6 and its membrane. (C) XRD patterns of LLZTO and its membrane. (D) Arrhenius plot of $\text{Li}_6\text{PS}_5\text{Cl}$ powder and its membrane. (E) Arrhenius plot of Li_3InCl_6 powder and its membrane. (F) Arrhenius plot of a PP membrane with nonflammable liquid electrolytes in comparison with an LLZTO membrane with nonflammable liquid electrolytes.

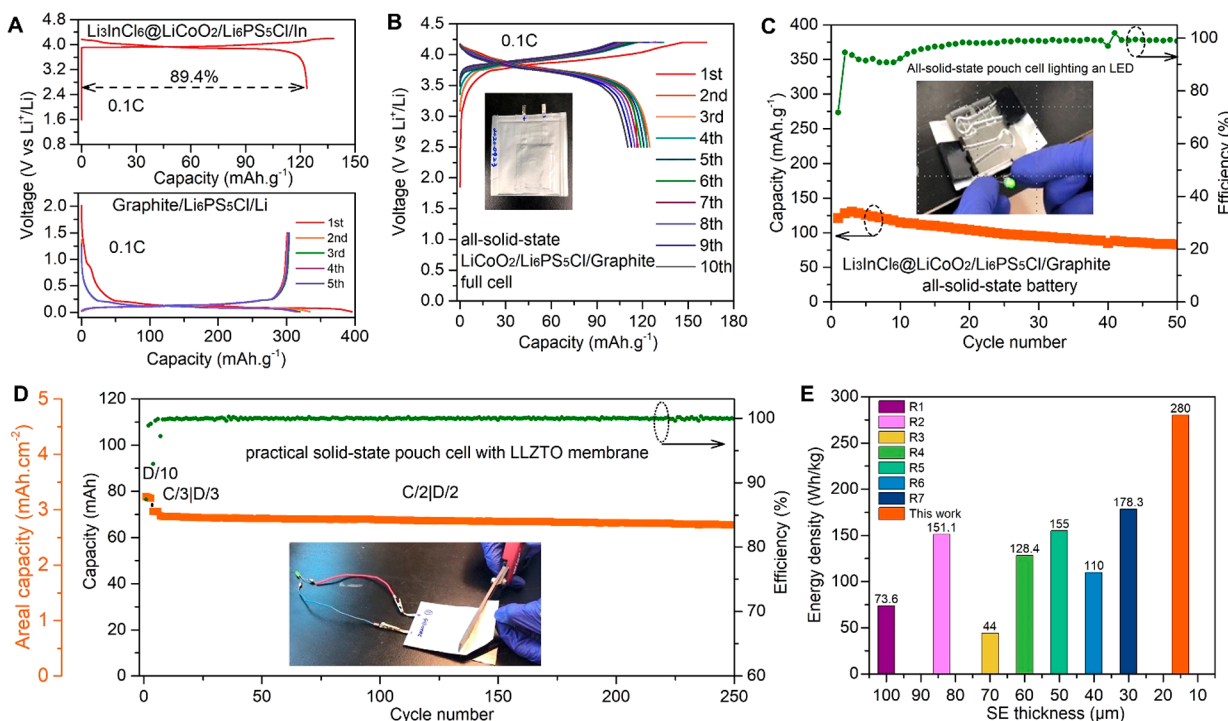


Figure 4. Electrochemical performance of all-solid-state pouch cells based on inorganic solid electrolyte membranes. (A) Initial charge-discharge curves of the freestanding electrode $\text{Li}_3\text{InCl}_6@\text{LiCoO}_2$ (top) and initial 5 charge-discharge curves of Graphite@ $\text{Li}_6\text{PS}_5\text{Cl}$ electrodes (bottom). (B) Initial 10 charge-discharge curves of ASSBs with a configuration of $\text{Li}_3\text{InCl}_6@\text{LiCoO}_2/\text{Li}_3\text{InCl}_6+\text{Li}_6\text{PS}_5\text{Cl}/\text{Graphite}@\text{Li}_6\text{PS}_5\text{Cl}$ and (C) their cycling stability at room temperature. (D) Cycling performance of oxide-based solid-state pouch cells with the LLZTO membrane. It should be mentioned that the nonflammable electrolyte was introduced to construct ionic contacts. (E) Energy density comparison.

For the 20 μm LLZTO membrane, its high ionic conductivity cannot be measured via simply cold pressing because of its mechanical stiffness. Using a high-temperature sintering process can realize its high ionic conductivity but the flexibility of the membrane will lose. On the other hand, our recent nail penetration test indicates that the commercial PP separator is the weakest part of large-capacity pouch cells.⁴³ Therefore, replacing the polymeric PP separator with thermally stable counterparts is believed to be an effective solution to improve battery safety. On consideration of its good flexibility and proper porosity (40–45%), this ultrathin LLZTO membrane can be used as an ideal ceramic separator with exceptional thermal stability (Figure S4). Video S1 records the flame test of a commercial PP separator, which is shrinkable and flammable. In contrast, the inorganic solid–solid LLZTO membrane is nonflammable, and no shrinkage occurs during the flame test (Video S2). To establish lithium-ion transport pathways between LLZTO membranes and electrodes, the common strategy is to add some liquid electrolytes or soft polymer electrolytes.^{44,45} However, conventional carbonate liquid electrolytes (1 mol L⁻¹ LiPF₆ in EC/EMC/DMC (1/1/1)) and polymer electrolytes are flammable as well (Video S3), which compromise the safety of ASSBs if they are added. To avoid this issue, a novel in-house-developed nonflammable electrolyte (1 mol LiTFSI in 90% sulfolane and 10% FEC) with a room-temperature ionic conductivity of 2.785 mS cm⁻¹ was developed (Figure S5 and Video S4). In conjunction with LLZTO membranes, the ionic conductivity can reach 0.52 mS cm⁻¹ (Figure 3F), which is comparable to that of a traditional polypropylene (PP) separator with the nonflammable electrolyte (0.56 mS cm⁻¹). Therefore, solid-state pouch cells can be realized using LLZTO membranes as ceramic separators in the combination of the nonflammable electrolytes, which also can enhance battery safety without compromising energy density.

All-solid-state pouch cells with dimensions of 30 mm \times 30 mm based on bilayer Li₃InCl₆ and Li₆PS₅Cl membranes were demonstrated. Li₃InCl₆ was used as the catholyte due to its high-voltage stability (>4.2 V vs Li⁺/Li).^{46,47} Therefore, the Li₃InCl₆@LiCoO₂ sheet electrode was also fabricated by the solvent-free process (Figure S6). The Li₃InCl₆@LiCoO₂ sheet electrode delivers a high capacity of 124.3 mAh g⁻¹ with a high Coulombic efficiency of 89.4% (Figure 4A). Similarly, the graphite@Li₆PS₅Cl sheet electrode was fabricated and delivered an initial discharge capacity of 395.6 mAh g⁻¹ and stabilized at 320 mAh g⁻¹ (Figure 4A). The initial Coulombic efficiency is 76.1%, which is due to the Li₆PS₅Cl decomposition by the graphite.⁴⁸ All-solid-state pouch cells with a configuration of Li₃InCl₆@LiCoO₂/Li₃InCl₆+Li₆PS₅Cl/Graphite@Li₆PS₅Cl show an initial capacity of 121.2 mAh g⁻¹ and a Coulombic efficiency of 71.8% (Figure 4B). The capacity was retained at 83.1 mAh g⁻¹ after 50 cycles (Figure 4C). The fabricated pouch cells can successfully light an LED, as shown in the image inserted in Figure 4C. The successful demonstration of all-solid-state pouch cells indicates that this dry electrode/electrolyte technology holds great promise for engineering all-solid-state pouch cells with inorganic solid electrolytes.

Using the LLZTO membranes as a ceramic separator, practical pouch cells with high-capacity electrodes (NMC811 (17.1 mg cm⁻²) and Si-C-450 (8.02 mg cm⁻²)) were demonstrated. As shown in Figure 4D, the initial discharge capacity is 77.6 mAh (188.8 mAh g⁻¹) at 0.1 C (1 C = 200 mA g⁻¹) and the corresponding areal capacity is 3.094 mAh cm⁻². Moreover, 71.3 mAh (173.6 mAh g⁻¹) was discharged at C/3

and 69.2 mAh (168.3 mAh g⁻¹) was obtained at 0.5 C. Furthermore, a high capacity of 65.3 mAh (158.9 mAh g⁻¹) was retained after 250 cycles. The corresponding capacity retention is as high as 94.4%. The estimated energy density of this LLZTO-based pouch cell can reach 280 Wh kg⁻¹, which represents the highest level among all the results reported so far (Figure 4E). In addition, this LLZTO-based pouch cell not only demonstrated good flexibility but also displayed unparalleled safety (Video S5 and Video S6). Impressively, it still can light an LED even when it is cut into small pieces (Video S7). The safety evaluation suggests using LLZTO membranes to replace conventional organic separators can significantly increase safety without compromising their energy density.

In summary, this work demonstrated a solvent-free method for fabricating solid-state pouch cells with ultrathin inorganic SE membranes. The solvent-free process is scalable, cost-effective, energy-efficient, environmentally friendly, and compatible with the existing roll-to-roll fabrication technology. Representative inorganic solid electrolytes, including oxide electrolytes (LLZTO), sulfide electrolytes (Li₆PS₅Cl), and halide electrolytes (Li₃InCl₆), were fabricated into freestanding membranes with a thickness of 15–20 μm and dimensions of 8 \times 6 cm². Their structure is just like that of a “gabion basket”, with all of the inorganic particles interwoven by PTFE fibers. Given its generality, this solvent-free method can be exploited further to fabricate other kinds of inorganic membranes, such as sodium-ion conductors (e.g., Na₃SbS₄) and common metal oxides (e.g., SiO₂). All-solid-state pouch cells with bilayer Li₃InCl₆ and Li₆PS₅Cl membranes were demonstrated and exhibited satisfactory electrochemical performance. Furthermore, LLZTO membrane-based pouch cells demonstrated not only superior electrochemical performance but also impressive safety. We believe the proposed solvent-free approach could be a viable technology that ensures a smooth transition of solid-state batteries from laboratory research to factory manufacturing, representing a substantial leap toward commercialization.

ASSOCIATED CONTENT

Supporting Information

The Supporting Information is available free of charge at <https://pubs.acs.org/doi/10.1021/acsenergylett.1c02261>.

Experimental method, energy density estimation, photos of SE membranes with different thicknesses, EIS spectra, flame test, ionic conductivity of the nonflammable electrolyte, photos of the all-solid-state pouch cell assembly, and additional tables as described in the text (PDF)

Flammability and shrinkage of commercial polypropylene (PP) separators (MP4)

Nonflammability of the inorganic ceramic LLZTO membrane (MP4)

Flammability of commercial carbonate liquid electrolytes (MP4)

Nonflammability of an innovative nonflammable electrolyte (MP4)

Oxide-based solid-state pouch cells demonstrating excellent flexibility (MP4)

Oxide-based solid-state pouch cells powering an electric fan (MP4)

LLZTO-based solid-state pouch cells showing excellent safety (MP4)

AUTHOR INFORMATION

Corresponding Authors

Jiantao Wang – China Automotive Battery Research Institute Co., Ltd, Beijing 101407, People's Republic of China;
Email: wangjt@glabat.com

Shangqian Zhao – China Automotive Battery Research Institute Co., Ltd, Beijing 101407, People's Republic of China;
Email: zhaosq@glabat.com

Huan Huang – Glabat Solid-State Battery Inc., London, Ontario N6G 4X8, Canada; Email: hhuang@glabat-ssb.com

Xueliang Sun – Department of Mechanical and Materials Engineering, University of Western Ontario, London, Ontario N6A 3K7, Canada; orcid.org/0000-0003-0374-1245; Email: xsun9@uwo.ca

Authors

Changhong Wang – Glabat Solid-State Battery Inc., London, Ontario N6G 4X8, Canada; Department of Mechanical and Materials Engineering, University of Western Ontario, London, Ontario N6A 3K7, Canada; orcid.org/0000-0002-4201-0130

Ruihui Yu – Department of Mechanical and Materials Engineering, University of Western Ontario, London, Ontario N6A 3K7, Canada

Hui Duan – Department of Mechanical and Materials Engineering, University of Western Ontario, London, Ontario N6A 3K7, Canada

Qingwen Lu – Glabat Solid-State Battery Inc., London, Ontario N6G 4X8, Canada; Department of Mechanical and Materials Engineering, University of Western Ontario, London, Ontario N6A 3K7, Canada

Qizheng Li – Glabat Solid-State Battery Inc., London, Ontario N6G 4X8, Canada

Keegan R. Adair – Department of Mechanical and Materials Engineering, University of Western Ontario, London, Ontario N6A 3K7, Canada

Danni Bao – Glabat Solid-State Battery Inc., London, Ontario N6G 4X8, Canada

Yang Liu – Glabat Solid-State Battery Inc., London, Ontario N6G 4X8, Canada

Rong Yang – China Automotive Battery Research Institute Co., Ltd, Beijing 101407, People's Republic of China

Complete contact information is available at:

<https://pubs.acs.org/10.1021/acsenergylett.1c02261>

Author Contributions

[†]C.W., R.Y., and H.D. contributed equally to this work.

Notes

The authors declare no competing financial interest.

ACKNOWLEDGMENTS

This work was supported by the Natural Sciences and Engineering Research Council of Canada (NSERC), Canada Research Chair Program (CRC), Canada Foundation for Innovation (CFI), Ontario Research Fund (ORF), China Automotive Battery Research Institute Co., Ltd., GLABAT Solid-State Battery Inc., and the University of Western Ontario.

REFERENCES

- (1) Li, M.; Lu, J.; Chen, Z.; Amine, K. 30 Years of Lithium-Ion Batteries. *Adv. Mater.* **2018**, *30* (33), 1800561.

(2) Wang, C.; Liang, J.; Zhao, Y.; Zheng, M.; Li, X.; Sun, X. All-solid-state lithium batteries enabled by sulfide electrolytes: from fundamental research to practical engineering design. *Energy Environ. Sci.* **2021**, *14* (5), 2577–2619.

(3) Zhang, J.; Zhao, J.; Yue, L.; Wang, Q.; Chai, J.; Liu, Z.; Zhou, X.; Li, H.; Guo, Y.; Cui, G.; Chen, L. Safety-Reinforced Poly(Propylene Carbonate)-Based All-Solid-State Polymer Electrolyte for Ambient-Temperature Solid Polymer Lithium Batteries. *Adv. Energy Mater.* **2015**, *5* (24), 1501082.

(4) Lin, D.; Yuen, P. Y.; Liu, Y.; Liu, W.; Liu, N.; Dauskardt, R. H.; Cui, Y. A Silica-Aerogel-Reinforced Composite Polymer Electrolyte with High Ionic Conductivity and High Modulus. *Adv. Mater.* **2018**, *30* (32), 1802661.

(5) Wu, J.; Rao, Z.; Cheng, Z.; Yuan, L.; Li, Z.; Huang, Y. Ultrathin, Flexible Polymer Electrolyte for Cost-Effective Fabrication of All-Solid-State Lithium Metal Batteries. *Adv. Energy Mater.* **2019**, *9* (46), 1902767.

(6) Zhao, Q.; Liu, X.; Stalin, S.; Khan, K.; Archer, L. A. Solid-state polymer electrolytes with in-built fast interfacial transport for secondary lithium batteries. *Nat. Energy* **2019**, *4* (5), 365–373.

(7) Kato, Y.; Hori, S.; Saito, T.; Suzuki, K.; Hirayama, M.; Mitsui, A.; Yonemura, M.; Iba, H.; Kanno, R. High-power all-solid-state batteries using sulfide superionic conductors. *Nat. Energy* **2016**, *1*, 16030.

(8) Lee, Y.-G.; Fujiki, S.; Jung, C.; Suzuki, N.; Yashiro, N.; Omoda, R.; Ko, D.-S.; Shiratsuchi, T.; Sugimoto, T.; Ryu, S.; Ku, J. H.; Watanabe, T.; Park, Y.; Aihara, Y.; Im, D.; Han, I. T. High-energy long-cycling all-solid-state lithium metal batteries enabled by silver–carbon composite anodes. *Nat. Energy* **2020**, *5* (4), 299–308.

(9) Peng, L.; Yu, C.; Zhang, Z.; Ren, H.; Zhang, J.; He, Z.; Yu, M.; Zhang, L.; Cheng, S.; Xie, J. Chlorine-rich lithium argyrodite enabling solid-state batteries with capabilities of high voltage, high rate, low-temperature and ultralong cyclability. *Chem. Eng. J.* **2022**, *430*, 132896.

(10) Duan, H.; Chen, W.-P.; Fan, M.; Wang, W.-P.; Yu, L.; Tan, S.-J.; Chen, X.; Zhang, Q.; Xin, S.; Wan, L.-J.; Guo, Y.-G. Building an Air Stable and Lithium Deposition Regulable Garnet Interface from Moderate-Temperature Conversion Chemistry. *Angew. Chem., Int. Ed.* **2020**, *59* (29), 12069–12075.

(11) Li, X.; Liang, J.; Yang, X.; Adair, K. R.; Wang, C.; Zhao, F.; Sun, X. Progress and perspectives on halide lithium conductors for all-solid-state lithium batteries. *Energy Environ. Sci.* **2020**, *13* (5), 1429–1461.

(12) Liang, J.; Li, X.; Wang, S.; Adair, K. R.; Li, W.; Zhao, Y.; Wang, C.; Hu, Y.; Zhang, L.; Zhao, S.; et al. Site-Occupation-Tuned Superionic $\text{Li}_x\text{ScCl}_3 + \text{x}$ Halide Solid Electrolytes for All-Solid-State Batteries. *J. Am. Chem. Soc.* **2020**, *142* (15), 7012–7022.

(13) Wang, S.; Bai, Q.; Nolan, A. M.; Liu, Y.; Gong, S.; Sun, Q.; Mo, Y. Lithium Chlorides and Bromides as Promising Solid-State Chemistries for Fast Ion Conductors with Good Electrochemical Stability. *Angew. Chem., Int. Ed.* **2019**, *58* (24), 8039–8043.

(14) Zhou, L.; Kwok, C. Y.; Shyamsunder, A.; Zhang, Q.; Wu, X.; Nazar, L. F. A new halospinel superionic conductor for high-voltage all solid state lithium batteries. *Energy Environ. Sci.* **2020**, *13* (7), 2056–2063.

(15) Wang, C.; Liang, J.; Luo, J.; Liu, J.; Li, X.; Zhao, F.; Li, R.; Huang, H.; Zhao, S.; Zhang, L.; Wang, J.; Sun, X. A universal wet-chemistry synthesis of solid-state halide electrolytes for all-solid-state lithium-metal batteries. *Sci. Adv.* **2021**, *7* (37), eabf1896.

(16) Cuan, J.; Zhou, Y.; Zhou, T.; Ling, S.; Rui, K.; Guo, Z.; Liu, H.; Yu, X. Borohydride-Scaffolded Li/Na/Mg Fast Ionic Conductors for Promising Solid-State Electrolytes. *Adv. Mater.* **2019**, *31* (1), 1803533.

(17) Lü, X.; Howard, J. W.; Chen, A.; Zhu, J.; Li, S.; Wu, G.; Dowden, P.; Xu, H.; Zhao, Y.; Jia, Q. Antiperovskite Li_3OCl Superionic Conductor Films for Solid-State Li-Ion Batteries. *Adv. Sci.* **2016**, *3* (3), 1500359.

(18) Chen, L.; Li, Y.; Li, S.-P.; Fan, L.-Z.; Nan, C.-W.; Goodenough, J. B. PEO/garnet composite electrolytes for solid-state lithium batteries: From “ceramic-in-polymer” to “polymer-in-ceramic”. *Nano Energy* **2018**, *46*, 176–184.

- (19) Cheng, Z.; Liu, T.; Zhao, B.; Shen, F.; Jin, H.; Han, X. Recent advances in organic-inorganic composite solid electrolytes for all-solid-state lithium batteries. *Energy Storage Mater.* **2021**, *34*, 388–416.
- (20) Tan, D. H. S.; Chen, Y.-T.; Yang, H.; Bao, W.; Sreenarayanan, B.; Doux, J.-M.; Li, W.; Lu, B.; Ham, S.-Y.; Sayahpour, B.; Scharf, J.; Wu, E. A.; Deysher, G.; Han, H. E.; Hah, H. J.; Jeong, H.; Lee, J. B.; Chen, Z.; Meng, Y. S. Carbon-free high-loading silicon anodes enabled by sulfide solid electrolytes. *Science* **2021**, *373* (6562), 1494–1499.
- (21) Yang, X.; Adair, K. R.; Gao, X.; Sun, X. Recent advances and perspectives on thin electrolytes for high-energy-density solid-state lithium batteries. *Energy Environ. Sci.* **2021**, *14*, 643–671.
- (22) Balaish, M.; Gonzalez-Rosillo, J. C.; Kim, K. J.; Zhu, Y.; Hood, Z. D.; Rupp, J. L. M. Processing thin but robust electrolytes for solid-state batteries. *Nat. Energy* **2021**, *6*, 227–239.
- (23) Wu, J.; Yuan, L.; Zhang, W.; Li, Z.; Xie, X.; Huang, Y. Reducing the thickness of solid-state electrolyte membranes for high-energy lithium batteries. *Energy Environ. Sci.* **2021**, *14* (1), 12–36.
- (24) Loho, C.; Djenicic, R.; Bruns, M.; Clemens, O.; Hahn, H. Garnet-Type Li₇La₃Zr₂O₁₂ Solid Electrolyte Thin Films Grown by CO₂-Laser Assisted CVD for All-Solid-State Batteries. *J. Electrochem. Soc.* **2017**, *164* (1), A6131–A6139.
- (25) Jiang, Z.; Wang, S.; Chen, X.; Yang, W.; Yao, X.; Hu, X.; Han, Q.; Wang, H. Tape-Casting Li_{0.34}La_{0.56}TiO₃ Ceramic Electrolyte Films Permit High Energy Density of Lithium-Metal Batteries. *Adv. Mater.* **2020**, *32* (6), 1906221.
- (26) Zhang, M.; Huang, Z.; Cheng, J.; Yamamoto, O.; Imanishi, N.; Chi, B.; Pu, J.; Li, J. Solid state lithium ionic conducting thin film Li_{1.4}Al_{0.4}Ge_{1.6}(PO₄)₃ prepared by tape casting. *J. Alloys Compd.* **2014**, *590*, 147–152.
- (27) Fu, K.; Gong, Y.; Hitz, G. T.; McOwen, D. W.; Li, Y.; Xu, S.; Wen, Y.; Zhang, L.; Wang, C.; Pastel, G.; Dai, J.; Liu, B.; Xie, H.; Yao, Y.; Wachsman, E. D.; Hu, L. Three-dimensional bilayer garnet solid electrolyte based high energy density lithium metal–sulfur batteries. *Energy Environ. Sci.* **2017**, *10* (7), 1568–1575.
- (28) Yang, C.; Zhang, L.; Liu, B.; Xu, S.; Hamann, T.; McOwen, D.; Dai, J.; Luo, W.; Gong, Y.; Wachsman, E. D.; Hu, L. Continuous plating/stripping behavior of solid-state lithium metal anode in a 3D ion-conductive framework. *Proc. Natl. Acad. Sci. U. S. A.* **2018**, *115* (15), 3770–3775.
- (29) Whiteley, J. M.; Taynton, P.; Zhang, W.; Lee, S.-H. Ultra-thin Solid-State Li-Ion Electrolyte Membrane Facilitated by a Self-Healing Polymer Matrix. *Adv. Mater.* **2015**, *27* (43), 6922–6927.
- (30) Zhao, C.-Z.; Chen, P.-Y.; Zhang, R.; Chen, X.; Li, B.-Q.; Zhang, X.-Q.; Cheng, X.-B.; Zhang, Q. An ion redistributor for dendrite-free lithium metal anodes. *Sci. Adv.* **2018**, *4* (11), eaat3446.
- (31) Wan, J.; Xie, J.; Kong, X.; Liu, Z.; Liu, K.; Shi, F.; Pei, A.; Chen, H.; Chen, W.; Chen, J.; Zhang, X.; Zong, L.; Wang, J.; Chen, L.-Q.; Qin, J.; Cui, Y. Ultrathin, flexible, solid polymer composite electrolyte enabled with aligned nanoporous host for lithium batteries. *Nat. Nanotechnol.* **2019**, *14* (7), 705–711.
- (32) Nam, Y. J.; Oh, D. Y.; Jung, S. H.; Jung, Y. S. Toward practical all-solid-state lithium-ion batteries with high energy density and safety: Comparative study for electrodes fabricated by dry- and slurry-mixing processes. *J. Power Sources* **2018**, *375*, 93–101.
- (33) Jung, W. D.; Jeon, M.; Shin, S. S.; Kim, J.-S.; Jung, H.-G.; Kim, B.-K.; Lee, J.-H.; Chung, Y.-C.; Kim, H. Functionalized Sulfide Solid Electrolyte with Air-Stable and Chemical-Resistant Oxysulfide Nano-layer for All-Solid-State Batteries. *ACS Omega* **2020**, *5* (40), 26015–26022.
- (34) Ruhl, J.; Rieger, L. M.; Ghidiu, M.; Zeier, W. G. Impact of Solvent Treatment of the Superionic Argyrodite Li₆PSSCl on Solid-State Battery Performance. *Adv. Energy Sustainability Res.* **2021**, *2*, 2000077.
- (35) Hippauf, F.; Schumm, B.; Doerfler, S.; Althues, H.; Fujiki, S.; Shiratsuchi, T.; Tsujimura, T.; Aihara, Y.; Kaskel, S. Overcoming binder limitations of sheet-type solid-state cathodes using a solvent-free dry-film approach. *Energy Storage Mater.* **2019**, *21*, 390–398.
- (36) Cangaz, S.; Hippauf, F.; Reuter, F. S.; Doerfler, S.; Abendroth, T.; Althues, H.; Kaskel, S. Enabling High-Energy Solid-State Batteries with Stable Anode Interphase by the Use of Columnar Silicon Anodes. *Adv. Energy Mater.* **2020**, *10* (34), 2001320.
- (37) Jiang, T.; He, P.; Wang, G.; Shen, Y.; Nan, C.-W.; Fan, L.-Z. Solvent-Free Synthesis of Thin, Flexible, Nonflammable Garnet-Based Composite Solid Electrolyte for All-Solid-State Lithium Batteries. *Adv. Energy Mater.* **2020**, *10* (12), 1903376.
- (38) Randau, S.; Weber, D. A.; Kötz, O.; Koerver, R.; Braun, P.; Weber, A.; Ivers-Tiffée, E.; Adermann, T.; Kulisch, J.; Zeier, W. G.; Richter, F. H.; Janek, J. Benchmarking the performance of all-solid-state lithium batteries. *Nat. Energy* **2020**, *5* (3), 259–270.
- (39) Zhu, G.-L.; Zhao, C.-Z.; Peng, H.-J.; Yuan, H.; Hu, J.-K.; Nan, H.-X.; Lu, Y.; Liu, X.-Y.; Huang, J.-Q.; He, C.; Zhang, J.; Zhang, Q. A Self-Limited Free-Standing Sulfide Electrolyte Thin Film for All-Solid-State Lithium Metal Batteries. *Adv. Funct. Mater.* **2021**, *31* (32), 2101985.
- (40) Tan, D. H. S.; Banerjee, A.; Chen, Z.; Meng, Y. S. From nanoscale interface characterization to sustainable energy storage using all-solid-state batteries. *Nat. Nanotechnol.* **2020**, *15* (3), 170–180.
- (41) Riphaus, N.; Strobl, P.; Stiaszny, B.; Zinkevich, T.; Yavuz, M.; Schnell, J.; Indris, S.; Gasteiger, H. A.; Sedlmaier, S. J. Slurry-Based Processing of Solid Electrolytes: A Comparative Binder Study. *J. Electrochem. Soc.* **2018**, *165* (16), A3993–A3999.
- (42) Yamamoto, M.; Terauchi, Y.; Sakuda, A.; Takahashi, M. Binder-free sheet-type all-solid-state batteries with enhanced rate capabilities and high energy densities. *Sci. Rep.* **2018**, *8* (1), 1212.
- (43) Qi, X.; Liu, B.; Pang, J.; Yun, F.; Wang, R.; Cui, Y.; Wang, C.; Doyle-Davis, K.; Xing, C.; Fang, S.; Quan, W.; Li, B.; Zhang, Q.; Wu, S.; Liu, S.; Wang, J.; Sun, X. Unveiling micro internal short circuit mechanism in a 60 Ah high-energy-density Li-ion pouch cell. *Nano Energy* **2021**, *84*, 105908.
- (44) Jaumaux, P.; Wu, J.; Shanmukaraj, D.; Wang, Y.; Zhou, D.; Sun, B.; Kang, F.; Li, B.; Armand, M.; Wang, G. Non-Flammable Liquid and Quasi-Solid Electrolytes toward Highly-Safe Alkali Metal-Based Batteries. *Adv. Funct. Mater.* **2021**, *31*, 2008644.
- (45) Wang, C.; Sun, Q.; Liu, Y.; Zhao, Y.; Li, X.; Lin, X.; Banis, M. N.; Li, M.; Li, W.; Adair, K. R.; Wang, D.; Liang, J.; Li, R.; Zhang, L.; Yang, R.; Lu, S.; Sun, X. Boosting the performance of lithium batteries with solid-liquid hybrid electrolytes: Interfacial properties and effects of liquid electrolytes. *Nano Energy* **2018**, *48*, 35–43.
- (46) Wang, C.; Liang, J.; Jiang, M.; Li, X.; Mukherjee, S.; Adair, K.; Zheng, M.; Zhao, Y.; Zhao, F.; Zhang, S.; Li, R.; Huang, H.; Zhao, S.; Zhang, L.; Lu, S.; Singh, C. V.; Sun, X. Interface-assisted in-situ growth of halide electrolytes eliminating interfacial challenges of all-inorganic solid-state batteries. *Nano Energy* **2020**, *76*, 105015.
- (47) Li, X.; Liang, J.; Luo, J.; Norouzi Banis, M.; Wang, C.; Li, W.; Deng, S.; Yu, C.; Zhao, F.; Hu, Y.; Sham, T.-K.; Zhang, L.; Zhao, S.; Lu, S.; Huang, H.; Li, R.; Adair, K. R.; Sun, X. Air-stable Li₃InCl₆ electrolyte with high voltage compatibility for all-solid-state batteries. *Energy Environ. Sci.* **2019**, *12* (9), 2665–2671.
- (48) Kim, D. H.; Oh, D. Y.; Park, K. H.; Choi, Y. E.; Nam, Y. J.; Lee, H. A.; Lee, S.-M.; Jung, Y. S. Infiltration of solution-processable solid electrolytes into conventional Li-ion-battery electrodes for all-solid-state Li-ion batteries. *Nano Lett.* **2017**, *17* (5), 3013–3020.